A thermo-fluid analysis in magnetic hyperthermia*

Iordana Astefanoaei[a)†], Ioan Dumitru[a)], Alexandru Stancu[a)], and Horia Chiriac[b)]

[a)] *Faculty of Physics, Alexandru Ioan Cuza University, Iasi, Romania*

[b)] *National Institute of Research & Development for Technical Physics, Iaşi, Romania*

(Received 27 July 2013; revised manuscript received 13 September 2013; published online 20 February 2014)

In the last years, hyperthermia induced by the heating of magnetic nanoparticles (MNPs) in an alternating magnetic field received considerable attention in cancer therapy. The thermal effects could be automatically controlled by using MNPs with selective magnetic absorption properties. In this paper, we analyze the temperature field determined by the heating of MNPs, injected in a malignant tissue, subjected to an alternating magnetic field. The main parameters which have a strong influence on temperature field are analyzed. The temperature evolution within healthy and tumor tissues are analyzed by finite element method (FEM) simulations in a thermo-fluid model. The cooling effect produced by blood flow in blood vessels from the tumor is considered. A thermal analysis is conducted under different distributions of MNP injection sites. The interdependence between the optimum dose of the nanoparticles and various types of tumors is investigated in order to understand their thermal effect on hyperthermia therapy. The control of the temperature field in the tumor and healthy tissues is an important step in the healing treatment.

Keywords: hyperthermia, magnetic nanoparticles, Bioheat equations

PACS: 44.10.+i, 44.05.+e, 87.85.J– **DOI:** 10.1088/1674-1056/23/4/044401

1. Introduction

In the living tissues, tumors occur when the cells multiply excessively. The cells growth can be benign or malignant. In the malignant tumor, the cells divide and grow uncontrollably invading surrounding tissues or spreading to other organs (metastasize) through the lymphatic system or bloodstream.[1,2] This kind of tumor is known as cancer and leads to the patient's death if untreated. In the benign tumor, the cells do not grow uncontrollably, nor invade neighboring tissues nor spread throughout the body.[3] The known therapies: radiotherapy, chemotherapy or hyperthermia each play an important role in healing patients. The hyperthermia used in addition to radiotherapy, chemotherapy, and surgery increases the survival prognostic of patients. The radiotherapy is commonly applied to the malignant tumors because of its ability to control cell growth.[1] Ionizing radiation destroys the DNA of exposed tissue.[2–4] Chemotherapy kills cancerous cells that divide rapidly.[2,3]

In hyperthermia, the tissue temperature increases by several degrees above the normal physiological level in a therapeutic temperature range of 42 °C–46 °C, activates enzymatic processes and determines the death of tumor cells because of their smaller thermal resistance. At a cellular level, the temperature increase improves the functionality of the cellular structures, affects the synthesis of nucleic acids and promotes changes in the conformation of DNA. Practically, the heat from a source stimulates the natural mechanisms of living tissue to fight and to destroy the malignant tissues, thereby protecting the normal cells from apoptosis.[2,5]

To increase the efficiency in the healing treatment by hyperthermia, a precise control of local temperature determined by a heat source within living tissue is required.

In the last few years, magnetic fluid hyperthermia (MFH) has become a promising method of heating target cancerous tissues. A fluid containing magnetic nanoparticles (MNPs) is injected into tumor.[6] The MNPs, placed in an external alternating magnetic field, generate heat through relaxation losses and transfer it to tissues and thus destroys the tumor cells.[7,8] For a specific MNP concentration this field must be chosen to be high enough to induce hyperthermia in the tumor but not exceed the safe limit for human exposure.[9,10] The local heating of the tumor reduces significantly the side effects in comparison with radiotherapy and chemotherapy.[11]

The MNPs with selective absorption properties which can transfer homogeneously the heat within living tissues are very good and promising candidates to be used in MFH.[12–15] Their use opens new horizons in the successful realization of the healing treatment.

The FeCrNbB system has special magnetic properties for its use in hyperthermia therapy.[12] The thermal response of the living tissues due to their being heated in alternative magnetic fields is studied in this paper. The high thermal characteristics (thermal conductivity and specific heat capacity) allow a good heat propagation and a rapid thermal response of the living tissues. The temperature field in the therapeutic range is mainly concentrated within tumor volume and more homogeneously distributed compared with other used materials (mag-

*Project supported by the Parteneriate HYPERTHERMIA (Grant No. 148/2012).

†Corresponding author. E-mail: iordana@uaic.ro

© 2014 Chinese Physical Society and IOP Publishing Ltd

netite, maghemite).

The conversion of the energy into heat is possible using several physical parameters (relaxation losses for smaller nanometer size) and its efficiency depends on several parameters such as size of particle, the characteristics and shape of the particle, and the alternating magnetic field amplitude.[12] An important task is to correlate the magnetic parameters with the AC field amplitude, frequency, and particle concentration in order to obtain the temperature within the therapeutic range.

In this paper, we investigate the temperature field induced by the heating of the MNPs within a primary liver cancer transited by the one or two significant blood vessels. Using a thermo-fluid model developed in Comsol Multiphysics, the thermal influence of blood flow in vessels with different sizes on temperature field within a tumor is studied. The FEM simulation allows the optimisation of the main parameters involved in the heating process of tissues. A better understanding of the thermal effects determined by the heating of MNPs in a magnetic field leads to the identification of the mechanism and the parameters which ensures the best healing treatment.

2. The thermo-fluid model

The control of temperature determined by an optimum dose of magnetic material concentrated in the small regions within the tumor is an important task in the MFH therapy. The optimum size of the injection sites and the minimum number of regions loaded with magnetic nanoparticles which ensures a temperature between 42 °C–46 °C in the tumor are another important focal point which must be solved by using a model.

The temperature field is computed in a geometry composed of a sphere-shaped tumor located in a cubic region from a healthy tissue. One or two significant blood vessels transit the tumor. The blood vessel can be an artery or a vein.

The size parameters of the analyzed geometry are a dimension of the cubic healthy region, blood vessel radius (R_v), and tumor diameter (d_t). The magnetic nanoparticles are concentrated in small spherical regions each with d_s diameter, assigned as injection sites. All computations are conducted for the $Fe_{67.7}Cr_{13}Nb_{0.3}B_{20}$ nanoparticle system.[12] When an alternating magnetic field with high frequency is applied, the MNPs loaded within the tumor absorb heat due to the relaxation processes in the superparamagnetic regime. The MNPs act as nanoheaters and the injection sites become the heating sources of the tumor. A suitable distribution of the injection sites can lead to the uniform heating of the tumor tissue.

The energy absorbed by the MNPs in the alternating magnetic field is[6,7,11]

$$P = \mu_0 \pi \chi_0 f \frac{2\pi f \tau_R}{1+(2\pi f \tau_R)^2} H^2, \tag{1}$$

where H is the field amplitude, f the field frequency, $\mu_0 = 4\pi \cdot 10^{-7}$ H/m the permeability and χ_0 the magnetic susceptibility

$$\chi_0 = \frac{\mu_0 M_s^2 V_M}{k_B T}.$$

Here, M_s is the saturation magnetization, V_M the particle volume, and $k_B = 1.38 \cdot 10^{-23}$ J/K the Boltzmann constant.

The heat described by expression (1) is attributed to the major relaxation processes: Brownian and Néel relaxation process in the superparamagnetic regime[6,11,15] The effective relaxation time is given by

$$\tau_R = \frac{\tau_N \tau_B}{\tau_N + \tau_B},$$

where Brownian relaxation time is

$$\tau_B = \frac{3\eta V_H}{k_B T}$$

and Néel relaxation time is

$$\tau_N = \tau_0 \frac{\sqrt{\pi}}{2} \frac{\exp(KV_M/k_B T)}{\sqrt{KV_M/k_B T}}.$$

Here, τ_0 is the average relaxation time, η the viscosity of the medium, and V_H the hydrodynamic volume of the MNPs.

Injection of the magnetic nanoparticles into the small regions of the tumor changes their thermal properties.[16] Their density, specific heat, and thermal conductivity become[17]

$$\rho_{mix} = \eta \rho_{MNP} + (1-\eta)\rho_{tumor}, \tag{2}$$

$$c_{mix} = \eta c_{MNP} + (1-\eta) c_{tumor}, \tag{3}$$

$$\frac{1}{k_{mix}} = \frac{\eta}{k_{MNP}} + \frac{1-\eta}{k_{tumor}}, \tag{4}$$

where η is the volume concentration of the MNPs. The physical properties are described by the following set of experimental data: the mass density: $\rho_{NMP} = 7060$ kg/m^3; the specific heat capacity: $c_{NMP} = 1227$ J/kg·K; the thermal conductivity: $k_{NMP} = 528$ W/mK; specific saturation magnetization: $M_s = 36$ emu/g.

The heat transfer in living tissues involves fundamental physical phenomena of conduction, convection, radiation, and metabolic heat production. The temperature values within tissues are obtained by solving Pennes bioheat equation[10,16]

$$\rho_t c_t \frac{\partial T}{\partial t} = \nabla(k_t \nabla T) + \rho_b w_b c_b (T_{art} - T) + Q_m + P \tag{5}$$

in Comsol Multiphysics by a finite element method (FEM), where ρ_t is the tissue density, c_t is the tissue specific heat, ρ_b the density of blood, c_b the blood specific heat, k_t the tissue thermal conductivity, w_b blood perfusion rate, T_{art} the arterial blood temperature, Q_m the metabolic heat source, and P the heat absorbed by the MNPs in the magnetic field at high frequency. This energy is transferred into tissues and contributes to the increase of the temperature. The presence of the blood vessels has a significant influence on the heat transfer in living tissues.[16] To investigate the thermal effects of blood vessels

on temperature fields of healthy and tumor tissues, the Navier–Stookes equation is solved[16]

$$\rho_b c_b \left(\frac{\partial T_b}{\partial t} + v_z \frac{\partial T_b}{\partial z} \right) = \nabla (k_b \nabla T_b) + P, \quad (6)$$

where k_b is the blood thermal conductivity and v_z is the blood velocity.[18] The second term on the left-hand side of Eq. (6) emphasizes the cooling effect of the blood vessels[16,18] which acts as a sink source within the tumor, contrary to the heating source. By controlling the heat-sink amount, the required local temperature could be obtained. This effect depends on the vessel size and blood velocity. The thermal influences of one or two significant vessels which transit the tumor are realistic and must be considered.

The blood in the vessel is considered as a Newtonian fluid in the laminar regime.[18] This is an accepted limitation of the model instead of the pulsatile blood flow.[16] Researchers[19] evaluated the effect of pulsatile blood flow in thermally significant blood vessels and they demonstrated that the pulsatile velocity profile produced little effect on the thermal lesion region of tissue and some minor differences in the thermal lesion region compared with a uniform or parabolic velocity profile.[16]

The temperature field in the tumour computed as a solution of Eqs. (5) and (6) depends on the following parameters:

i) size, thermal and magnetic properties;

ii) injection site distribution in the tumour;

iii) healthy and tumour thermal properties;

iv) the presence of the larger blood vessels in the tumour.

The interdependence between of these parameters and of their major role in the heating and destroying the process of tumours is an important point in the hyperthermia studies.

We now discuss the boundary conditions. In the numerical simulations the temperature field was computed for a spherical liver tumor of a 14-mm diameter embedded in a 30 mm × 30 mm × 30 mm cube of healthy liver tissue. The temperature, $T_0 = 37$ °C was considered on the external surface of the cube (Dirichlet boundary condition).

A larger blood vessel (BV) parallel to the z axis is considered to transit the middle tumour ($x = y = 0$) (Fig. 1). The flow velocity of blood along the z direction is $v_z = 2V_0 \left(1 - r_v^2/R_v^2\right)$, where r_v is the distance along the radial axis of the BV ($-R_v < r_v < R_v$, R_v is the radius of BV) and V_0 the center velocity of the blood. The flow velocity of blood along the x direction and y-coordinate value is considered to be zero ($v_x = v_y = 0$).[16]

At tumor–vessel interfaces, the Newman boundary conditions are imposed. The heat flux coming from the tumor is completely received by the BV. The continuity condition of the heat flux is imposed at the tumor–healthy region interface and tumor–injection site interfaces, too.

The tumor is loaded with nanoparticles at 16 injection sites each with a 0.7-mm diameter. The nanoparticles diameter is 10 nm and their mass concentration is $c = 10$ mg/cm^3. A spatial distribution of the injection sites is presented schematically in Fig. 1. In the plane *xoy* are distributed 8 injection sites (one injection site at every 45°), in the plane *zoy* are 4 injection sites, and the same in the plane *zox* (one injection site per 90°).

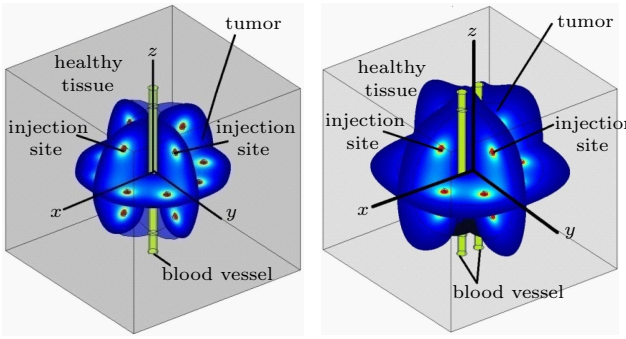


Fig. 1. (color online) Schematic distributions of the injection sites in a tumor from healthy region.

Due to the spherical symmetry, there is a natural tendency of the heat to accumulate at the tumour center. The injection sites are placed at the tumour periphery in an ordered distribution for each of the planes: *xoy*, *xoz*, and *yoz* (Fig. 1).

3. Results

For simulations, we have considered a liver tissue due to its complexity regarding the blood vessels distribution. This highly perfused organ contains three significant types of blood vessels: hepatic arteries, portal veins, and hepatic veins (with different diameters and flow velocities) and branches of arterioles, venule and capillaries.[20] A cancer which starts in the liver is called a primary liver cancer. For example, the hepatocellular carcinoma (HCC) contains different cell types: bile ducts and fat-storing cells and significant blood vessels such as arterioles or venules.

An alternating magnetic field with a frequency $f = 150$ kHz and a field amplitude $H = 5$ kA/m is considered. These values verify the criterion of exposure safe and tolerance for the ablation of the whole tumour according to Hergt condition,[9] $H \cdot f < 5 \cdot 10^9$. The power density P is $P = 5.75 \cdot 10^7$ W/m^3.

Figure 2 shows the temperature fields in the tumor transited by the one and two blood vessels respectively. Due to the cooling effect induced by the blood vessels within the tissue, the temperature values decrease suddenly in their vicinity. The temperature on the tumor boundary is very close to the therapeutic temperature. The healthy tissue is protected by excessive heating over normal temperature limit. The higher value of MNP thermal conductivity allows a good heat transfer within the tissue. As a consequence, the temperature in the tumor varies between 41 °C and 46 °C if one vessel transits

the tumour and between 40 °C and 46 °C if two blood vessels transits the tumor. An ordered distribution of the injection sites has temperature homogeneity in tissues.

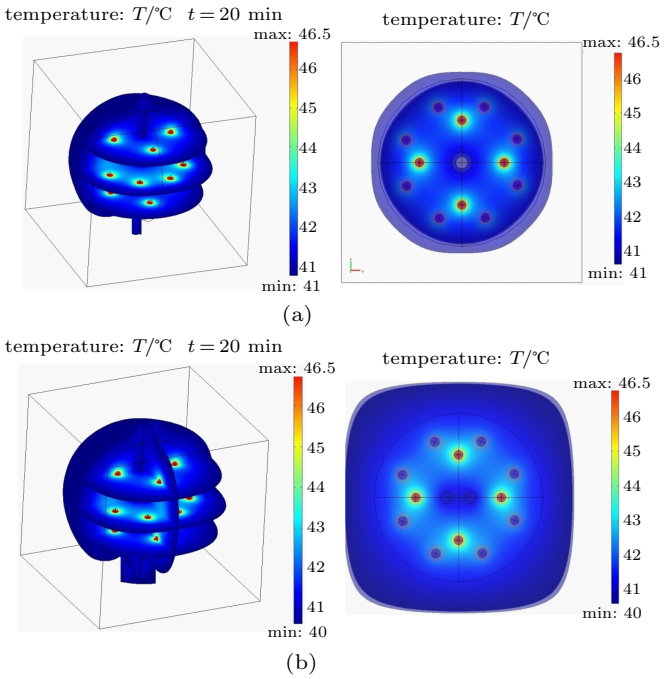


Fig. 2. (color online) Spatial temperature in the tumor at time $t = 20$ min. Panel (a) shows one blood vessel of 1-mm diameter transits the tumor, and panel (b) displays two blood vessels of 1-mm diameter at 1-mm distance transits the tumor.

Other MNPs are tested to verify the absorption properties and the corresponding thermal field in the tumor. The temperature values are computed by using FeCrNbB particles, maghemite and magnetite particles as magnetic materials. The magnetite and maghemite characteristics are considered as those in Ref. [21]. Figure 3 shows the temporal evolutions of temperature on the tumor boundary (Fig. 3(a)) and the temperature on the tumor diameter at the thermal equilibrium (Fig. 3(b)) for these magnetic materials.

As a general characteristic, the temperature value increases up to a saturation value, which corresponds to the thermal equilibrium of the tissue. The thermal field obtained for $Fe_{67.7}Cr_{13}Nb_{0.3}B_{20}$ nanoparticles reaches the thermal equilibrium in a shorter time than the one generated by maghemite or magnetite particles. Also, the temperature values due to maghemite and magnetite particles in the tumor are higher than the ones due to $Fe_{67.7}Cr_{13}Nb_{0.3}B_{20}$ nanoparticles. The cooling effect determined by the presence of a blood vessel within the tumor is much stronger if the maghemite and magnetite particles are used. A high difference between maximum temperature value and minimum temperature value in the tumor implies the presence of high thermal gradients in the tumor. The temperature values determined by $Fe_{67.7}Cr_{13}Nb_{0.3}B_{20}$ nanoparticles correspond to the therapeutic range. The $Fe_{67.7}Cr_{13}Nb_{0.3}B_{20}$ nanoparticles transfer the heat within the tumor more homogeneously thus keeping the temperature therapeutic range in the whole tumor volume.

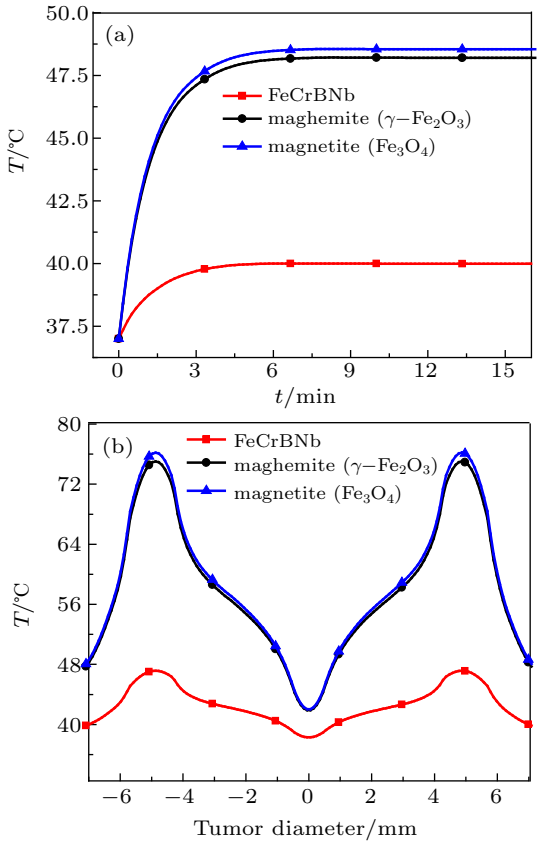


Fig. 3. (color online) Temperatures in the tumor for different magnetic materials: $Fe_{67.7}Cr_{13}Nb_{0.3}B_{20}$ nanoparticles, maghemite and magnetite nanoparticles. Panel (a) shows the time evolutions of temperature on the tumor boundary, and panel (b) displays variations of temperature with the tumor diameter at time $t = 20$ min.

Figure 4 shows the temperature fields in the different planes: *yox* and *yoz* within the tumor considering the configurations: a) no blood vessel transits the tumor, b) one blood vessel in the center, and c) two blood vessels in the *y* direction at distance 1 mm away from each other for the same particle and field parameters.

In Fig. 4(a) the model results for the temperature values in the tumor considers no blood vessels. The temperature in the tumor is approximately between 42 °C and 46 °C. The therapeutic temperature range reaches 97% of the tumor volume.

In Fig. 4(b) the temperature values are computed with consideration that one blood vessel of 1-mm diameter transits the tumor. The temperature decreases in the center of the tumor and the temperature therapeutic range is ensured on 90% of the tumor volume. The cooling effect is intensified if two blood vessels transit the tumor (Fig. 4(c)).

Figures 4(a)–4(c) show the possibilities of particles concentrated in 16 zones each with a 0.7-mm diameter to heat the tumor in the therapeutic temperature range homogeneously as required.

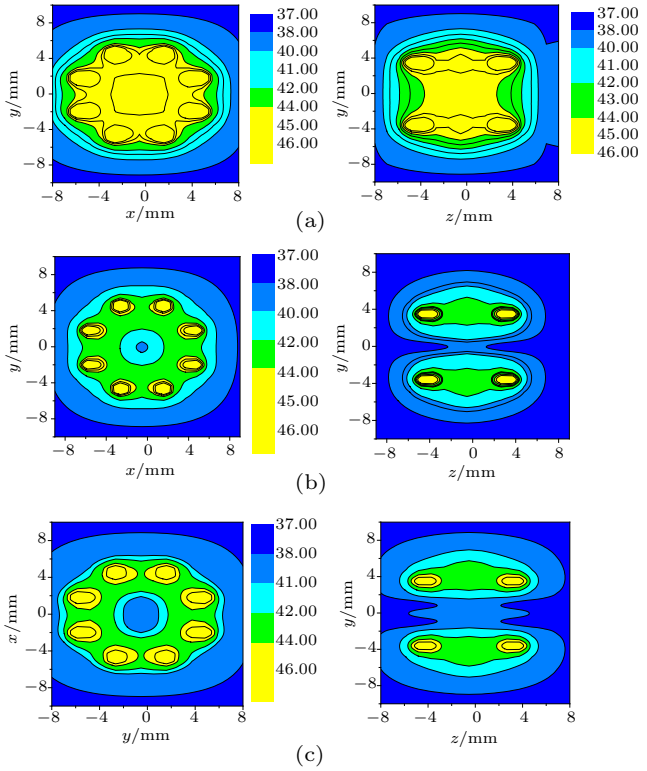


Fig. 4. (color online) Temperatures (°C) in the tumor for different configurations: (a) no blood vessels, (b) one blood vessel, and (c) two blood vessels.

The influences of the blood vessels on the tumor temperature are presented in Fig. 5. The temperature in the x direction is computed for three cases: (a) no blood vessel, (b) one significant blood vessel transits the tumor, and (c) two significant blood vessels in the tumor. It is observed that the temperature has a minimum value in the place where the BV is located. The presence of a BV in the tumor reduces the temperature in a large space in the tumor, around BV, where appears the possibility that locally the temperature is below that of the therapeutic range.

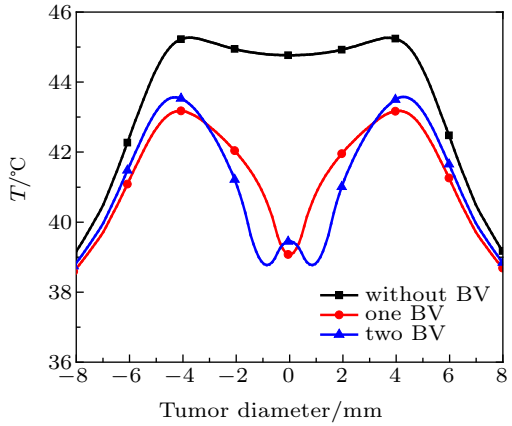


Fig. 5. (color online) Temperatures (°C) in the tumor in the ox direction for the following configurations: no blood vessels, one blood vessel, and two blood vessels.

The temperature of the therapeutic range is ensured by using the optimum particle concentration (Fig. 6). For two nanoparticle concentrations, the temperatures are computed for the same configurations: there are two blood vessels in the tumor. As a general characteristic, the tumor is uniformly heated in the therapeutic temperature range by a higher nanoparticle concentration. The cooling effect due to the presence of a vessel can be diminished for a higher nanoparticle concentration.

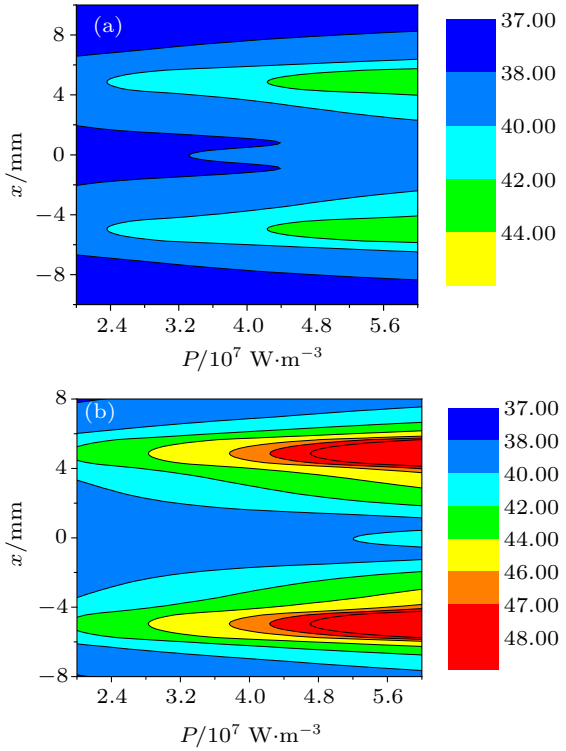


Fig. 6. (color online) Temperatures (°C) in the tumor in the x direction for two values of nanoparticles concentrations: (a) $c =$ 10 mg/cm^3 and (b) $c = 15$ mg/cm^3 in the same configurations of two blood vessels in tumor.

The nanoparticle concentration is a main parameter which needs to be optimized in order to obtain the therapeutic temperature range within the tumor.

A high MNP concentration leads to an increase of temperature in the tumor and a diminishing of the cooling effect of BV (Fig. 7).

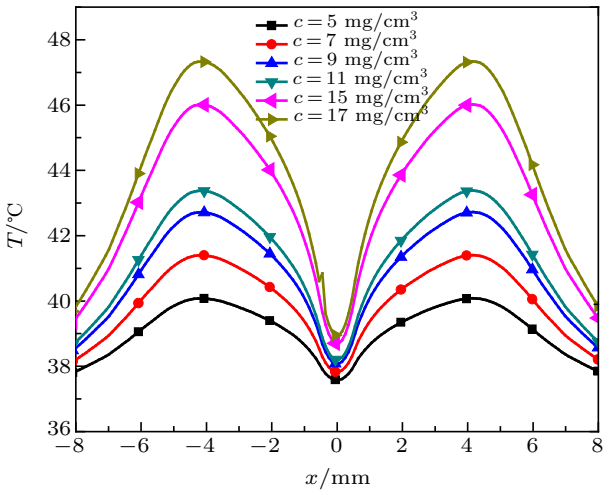


Fig. 7. (color online) Variations of temperature (°C) along the x direction for different values of nanoparticles concentrations.

Figure 8 shows the influence of vessel diameter on the tumor temperature field at the same blood flow rate. The temperature values in the tumor are smaller for larger vessel diameter. A larger blood vessel determines an increase of thermal heat loss and as a consequence the global tumor temperature decreases.

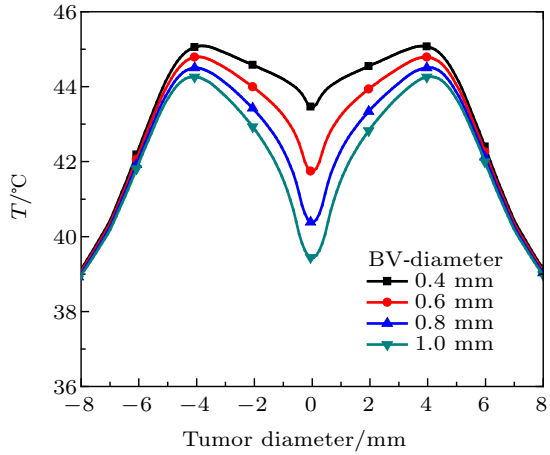


Fig. 8. (color online) Variations of temperature (°C) in the *x* direction with blood vessel diameter.

Figure 9 shows the temperature values in the *ox* direction with the tumor diameter for different blood velocities in the vessel. For a higher blood velocity, the temperature values decreases suddenly at the center of the tumor where it is considered the blood vessel. The cooling effect of the blood vessel is intensified by the higher blood velocity. A smaller value of blood velocity can maintain the therapeutic temperature in the tumor. The temperature value on the boundary is smaller if the blood velocity is higher because of the higher cooling effect of the vessel. The blood velocity in the vessel does not influence the time needed to reach the thermal equilibrium on the boundary.

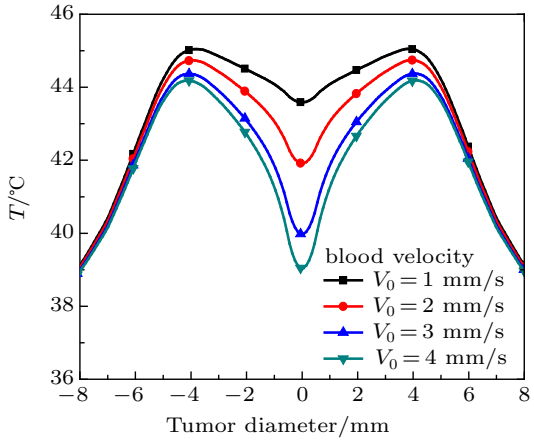


Fig. 9. (color online) Variations of temperature (°C) in the *x* direction with tumor diameter for different blood velocities.

In order to optimize the number of the injection sites within the tumor, the temperature values are computed within the tumor transited by one significant blood vessel. Considered is another arrangement of the injection sites, i.e., there are 4 injection sites in each of plans *xoy*, *xoz*, and *yoz*, so there are 12 injection sites of 0.9-mm diameter in total. The temperature values in the *y* direction for different values of power density are computed and compared for both injection site distributions (Fig. 10). The temperature in the central part of the tumor is higher if 16 zones of 0.7-mm diameter are used. Both configurations heat almost uniformly the tumor in the therapeutic temperature range.

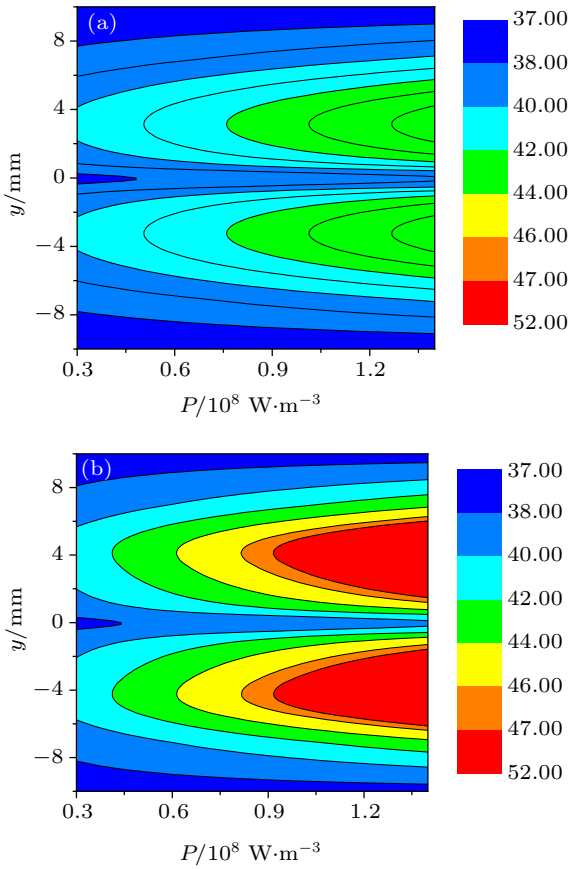


Fig. 10. (color online) Temperature contours (°C) in the *y* direction for different distributions of injection sites in tumor for (a) 12 injection zones each with a 0.9-mm diameter and (b) 16 injection zones each with a 0.7-mm diameter.

4. Discussion

The model developed in this paper is used to predict and optimize the temperature field determined by the magnetic nanoparticles injected into a tumor when the magnetic field is applied. Elaboration of a model is an important step for hyperthermia treatment planning. The model can be used as a planning tool to improve the quality of therapy. For each patient, an individual therapy planning is necessary in correlation with the tumor location, geometry, shape, and size. The first step of hyperthermia treatment planning is to elaborate a patient model by segmentation of images from computerized tomography or magnetic resonance imaging scans. This segmentation is used to compute the temperature field in the tumor located in a patient organ. The simulations allow i) the optimization of the main parameters which influence strongly the heating of the tumor in the therapeutic temperature range

and ii) the better control of temperature through treatment preplanning.

The FeCrNbB systems have capability to focus the heat within the volume of the tumor thereby protecting the normal tissue which surrounds the tumor from being impaired. These particles with high values of thermal conductivity and specific heat capacity determine a faster thermal response of the living tissues. The local and focused heating determines a more efficient control of the temperature within the tumor than other particles: maghemite or magnetite.

5. Conclusion

A good temperature control in the tumor can be obtained by using the magnetic $Fe_{67.7}Cr_{13}Nb_{0.3}B_{20}$ nanoparticles in hyperthermia therapy. For suitable magnetic field parameters such as intensity, frequency and tissue parameters, these particles have the capability to focus homogeneously the thermal field within the therapeutic range of temperature. The tumor boundary does not exceed the temperature range: 40 °C–42 °C and the healthy region is protected from overheating.

The heat absorbed by these particles in an alternating magnetic field is transferred faster in tissues and the thermal equilibrium is reached in a shorter time than other magnetic materials such as magnetite or maghemite. The results suggest a better control of the therapeutic results for the used dose in the case of these types of particles.

A magnetic field having frequency $f = 150$ kHz and the field amplitude $H = 5$ kA/m is required for a nanoparticle concentration of 10 mg/cm^3 injected into a tumor of 14-mm diameter to ensure the therapeutic temperature range. The cooling effect of the blood vessels is reduced for the vessels with smaller diameters. A smaller blood velocity diminishes the cooling effect.

A distribution of injection sites within the tumor must be obtained by taking into account the presence of paired vessels, their size, and blood velocities.

$Fe_{67.7}Cr_{13}Nb_{0.3}B_{20}$ nanoparticle hyperthermia induced magnetically is a promising tool which can be used successfully for removing tumors. The treatment efficacy could be improved by their use in hyperthermia technique.

References

[1] Aebersold D M 2009 *Liver International* **29** 145

[2] Chicel A, Skowronek J, Kubaszewska M and Kanikowski M 2007 *Reports of Practical Oncology and Radiotherapy* **12** 267

[3] He Y, Shirazaki M, Liu H, Himeno R and Sun Z 2006 *Computers in Biology and Medicine* **36** 1336

[4] Wust P, Hildebrandt B, Sreenivasa G, Rau B, Gellermann J, Riess H, Felix R and Schlag P M 2002 *Lancet Oncology* **3** 487

[5] Silva A C, Oliveira T R, Mamani J B, Malheiros S, Malavolta L, Pavon L F, Sibov T T, Amaro E, Tannús A, Vidoto L G, Martins M J, Santos R S and Gamarra L F 2011 *International Journal of Nanomedicine* **6** 591

[6] Maenoso S and Saita S 2006 *IEEE Trans. Magn.* **42** 1638

[7] Rosensweig R E 2002 *J. Magn. Magn. Mater.* **252** 370

[8] Pavel M, Gradinariu G and Stancu A 2008 *IEEE Trans. Magn.* **44** 11

[9] Hergt R and Dutz S 2007 *J. Magn. Magn. Mater.* **311** 187

[10] Pavel M and Stancu A 2009 *IEEE Trans. Magn.* **45** 4825

[11] Hergt R, Andra W, D'Ambly C G, Hilger I, Kaiser W A, Richter U and Schmidt H G 1998 *IEEE Trans. Magn.* **34** 3745

[12] Lupu N, Chiriac H, Corodeanu S and Ababei G 2011 *IEEE Trans. Magn.* **l4** 3794

[13] Atsarkin V A, Levkin L V, Posvyanskiy V S, Melnikov O V, Markelova M N, Gorbenko O Y and Kaul A R 2009 *International Journal of Hyperthermia* **25** 240

[14] Lee J H, Jang J, Choi J, Moon S H, Noh S, Kim J, Kim J G, Kim I S, Park K I and Cheon J 2011 *Nat. Nanotechnol.* **6** 418

[15] Zhang Y, Gu H C and Wang X M 2007 *J. Magn. Magn. Mater.* **311** 228

[16] Wang Q, Deng Z S and Liu J 2012 *Journal of Nanoparticle Research* **14** 974

[17] Andrä W, d'Ambly C G, Hergt R, Hilger I and Kaiser W A 1999 *J. Magn. Magn. Mater.* **194** 197

[18] Kolios M C, Sherar M D and Hunt J W 1995 *Phys. Med. Bio.* **40** 477

[19] Horng T L, Lin W L, Liauh C T and Shih T C 2007 *Med. Phys.* **34** 1312

[20] Thiriet M 2008 *Biology and Mechanics of Blood Flows,* Part II: *Mechanics and Medical Aspects* (New York: Springer) p. 20

[21] Pankhurst Q A, Connolly J, Jones S K and Dobson J 2003 *J. Phys. D: Appl. Phys.* **36** R167